Interaction of Tet Repressor with Operator DNA and with Tetracycline Studied by Infrared and Raman Spectroscopy

C. Krafft,* W. Hinrichs,# P. Orth,# W. Saenger,# and H. Welfle*
*Max-Delbrück-Centrum für Molekulare Medizin, D-13125 Berlin, and #Institut für Kristallographie, Freie Universität Berlin, D-14195 Berlin, Germany

ABSTRACT Tet repressor (TetR) is involved in the most abundant mechanism of tetracycline (Tc) resistance of Gram-negative bacteria. Raman spectra were measured for the class D TetR protein, for an oligodeoxyribonucleotide with sequence corresponding to operator site O1, and for the TetR:oligonucleotide complex. TetR forms a complex with $[Ni\text{-}Tc]^+$, which does not bind to operator DNA. Raman and infrared measurements indicate nearly identical conformations of TetR with and without $[Ni\text{-}Tc]^+$. Differences between the experimental spectrum of the TetR:operator DNA complex and the computed sum of the component spectra provide direct spectroscopic evidence for changes in DNA backbone torsions and base stacking, rearrangement of protein backbone, and specific contacts between TetR residues and DNA bases. Complex formation is connected with intensity decrease at 1376 cm^{-1} (participation of thymine methyl groups), intensity increase at 1467 cm^{-1} (hydrogen bond formation at guanine N7), decreased intensity ratio I_{854}/I_{823} (increased hydrophobicity of tyrosine environment), increased intensity at 1363 cm^{-1} (increased hydrophobicity of tryptophan ring environment), differences in the range 670–833 cm^{-1} (changes in B-DNA backbone torsions and base stacking), and decreased intensity of the amide I band (structural rearrangement of TetR backbone consistent with a reduction of the distance between the two binding helices).

INTRODUCTION

The most abundant resistance mechanism against tetracyclines in Gram-negative bacteria is based on the active export of tetracycline (Tc) out of the cytoplasm by the intrinsic membrane protein TetA (Kaneko et al., 1985; Yamaguchi et al., 1990). The expression of the latter is regulated by tetracycline repressor (TetR). Two homodimeric TetR molecules bind with α-helix-turn-α-helix (HTH) motifs to two tandemly oriented DNA operator regions of the resistance determinant, named O1 and O_2, thereby blocking the expression of two genes, one encoding for TetA and the other for TetR. Tc, in complex with divalent metal ions (M^{2+}), forms a very stable complex with TetR that cannot bind to the operators. Consequently, in the presence of Tc and M^{2+}, the expression of TetR and TetA is induced, and after insertion of TetA in the cytoplasmic membrane, Tc is exported into the periplasm before it can inhibit ribosomal activity.

The crystal structure of the complex between TetR of class D ($TetR^D$), Tc, and a Mg^{2+} ion was determined by multiple isomorphous replacement at 2.5-Å resolution (Hinrichs et al., 1994; Kisker et al., 1995). TetR forms stable homodimers, the polypeptide chain of a monomer being folded into 10 α-helices. The N-terminal three-helix bundle of each monomer represents the DNA-binding domain with typical HTH motif. In the TetR:$[Mg\text{-}Tc]^+$ complex, the two recognition helices are 39 Å apart. Because the distance between two consecutive major grooves of B-DNA, to which Tc free TetR binds, is only 34 Å, the induced TetR is unable to attach to the operators O1 and O2.

The DNA-binding properties of TetR were extensively analyzed (Helbl et al., 1995, and references cited therein). The ability of mutant repressors to bind to operator variants was studied by constructing TetR mutants with single amino acid residue replacements at eight positions (Thr^{27}, Arg^{28}, Gln^{38}, Pro^{39}, Thr^{40}, Tyr^{42}, Trp^{43}, His^{44}) within the HTH motif (Baumeister et al., 1992). Five contacts between repressor monomer and operator half-site were proposed, including two H-bonds of Arg^{28} to guanine of the G·C base pair at operator position 2, two H-bonds of Gln^{38} to adenine of the A·T base pair at position 3, van der Waals contact of the methyl group of Thr^{40} with cytosine of the G·C base pair at position 6, and the insertion of the methylene groups of the side chain of Pro^{39} between the methyl groups of the thymines of T·A and A·T base pairs at positions 4 and 5 of the *tet* operator (Baumeister et al., 1992). Computer modeling, using the canonical structures of the HTH motif and B-DNA, supported the proposed contacts (Baumeister et al., 1992). For a long time it was difficult to obtain direct experimental evidence for these interactions, because of the lack of crystals of the TetR:operator complex suitable for a high-resolution x-ray structural determination.

A direct physicochemical approach to the study of the TetR-DNA interaction was undertaken with fluorescence spectroscopy (Peviani et al., 1995, and references cited therein). TetR contains two tryptophan residues at positions 43 and 75. From TetR wild-type and mutant (Trp^{43} and Trp^{75} exchange against Phe, respectively) studies, it was concluded that Trp^{75} is located within a hydrophobic environment in the vicinity of the binding site of the inducer Tc.

Received for publication 3 June 1997 and in final form 22 October 1997.
Address reprint requests to Dr. Heinz Welfle, Max-Delbrück-Centrum für Molekulare Medizin, Robert-Rössle-Strasse 10, D-13125 Berlin, Germany. Tel.: 49-30-9406-2840; Fax: 49-30-9406-2840; E-mail: welfle@orion.rz.mdc-berlin.de.

0006-3495/98/01/63/09 $2.00

Trp^{43} belongs to the HTH motif, is solvent exposed in the free protein, and participates in the operator binding.

Raman spectroscopy is well suited to probing the structure of nucleoprotein complexes (Thomas and Tsuboi, 1993) and was applied to the study of several repressor-operator systems (Benevides et al., 1991b,c, 1994a,b). Here we employ infrared and Raman spectroscopy to investigate the solution structure of TetR and study the TetR:operator complex by Raman spectroscopy. The results are discussed in relation to the proposed molecular model of the TetR:operator complex (Baumeister et al., 1992) and provide spectroscopic evidence for some of the contacts proposed by genetic experiments.

MATERIALS AND METHODS

Tet repressor protein, operator DNA, tetracycline, and complex formation

Overproduction from *Escherichia coli* strains and purification of $TetR^D$ were performed as described (Ettner et al., 1996). Protein concentrations were determined using an extinction coefficient at 280 nm of 18,700 M^{-1} cm^{-1}. The protein was dissolved at 23 $\mu g/\mu l$ in 50 mM Tris-HCl buffer, pH 8.0. For measurements in D_2O, the protein was lyophilized and redissolved in the appropriate volume of D_2O.

Oligodeoxyribonucleotides were purchased from Tib Molbiol (Berlin, Germany) and further purified by fast protein liquid chromatography (Pharmacia, Uppsala, Sweden) and standard procedures. The sequences of the 17-mer operator DNA (molecular mass 10,400 Da) and the 18-mer operator DNA (molecular mass 11,000 Da) are shown in Fig. 1. The 17-mer operator DNA corresponds to the nucleotide sequence of operator O1. The 18-mer operator DNA contains one additional unpaired thymine at each 3′ end. These sequences were chosen for Raman studies because of the promising results obtained in crystallization experiments with their TetR complexes (Orth et al., 1998). Concentrations were determined using an extinction coefficient at 260 nm of 22.5 $ml \cdot mg^{-1} \cdot cm^{-1}$. Equimolar amounts of each strand were mixed and annealed by heating to 80°C in a dry bath, followed by slow cooling. The duplex was lyophilized and redissolved at a concentration of 17 $\mu g/\mu l$ in 100 mM NaCl, 20 mM Tris-HCl, pH 7.5.

Tetracycline (tetracycline hydrochloride, molecular mass 480.9 Da) was purchased from Boehringer Mannheim (Mannheim, Germany) and used without further purification. A 5 mM stock solution was prepared in 50 mM Tris-HCl, 5 mM $NiCl_2$, pH 8.0. Ni^{2+} was used instead of Mg^{2+} because it quenches fluorescence, a prerequisite for Raman experiments. The TetR:$[Ni\text{-}Tc]^+$ complex was prepared by mixing of equimolar amounts of the components. Tc binds with high affinity to TetR when Mg^{2+} is substituted by Ni^{2+}. Complexes of Tc with divalent heavy metal ions are much stronger inducers of TetR compared to $[Mg\text{-}Tc]^+$. This was shown in detail for $[Fe\text{-}Tc]^+$ (Ettner et al., 1995). The structures of the TetR:$[Ni\text{-}Tc]^+$ complex and other complexes containing 3d-metal ions instead of Mg^{2+} were solved by single-crystal x-ray diffraction studies (Orth et al., 1997, unpublished results).

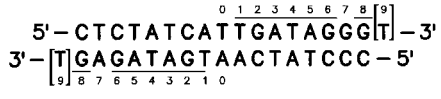

FIGURE 1 Nucleotide sequence of the 17-mer and the 18-mer *tet* operators. The palindromic part is underlined. The central base pair is numbered zero. The unpaired thymines in positions 9 at the 3′ ends of the 18-mer operator are shown in brackets.

TetR:operator complexes were prepared by mixing appropriate amounts of the components to produce a 1:1 molar ratio of TetR dimer to operator duplex.

Raman spectroscopy

Approximately 12 μl solution was pipetted into homemade cuvettes. These cuvettes consist of cylindrical quartz bodies with quartz bottoms and Teflon stoppers. For the recording of Raman spectra, the samples were excited with the 488-nm line of an Innova 90 argon laser (Coherent, Santa Clara, CA). The measurements were repeated with 514.5-mm excitation. Interference filters eliminated plasma lines. Solutions were measured in the macro chamber of the spectrometer T64000 (Jobin Yvon, France) with a 90° setup. The excitation energy at the sample was ~100 mW. Rayleigh scattering was separated by Notch filters, and Raman scattering was recorded with a liquid nitrogen-cooled CCD detector. The room temperature was held constant at 23°C. Ten spectral scans of 20 s each at four spectrometer positions were averaged for the region 600-1720 cm^{-1} to enhance the signal-to-noise ratio.

Raman data analysis, including buffer subtraction and background correction, was performed with the software package Spectramax (Jobin Yvon) supplemented by some of our own programs. Solution spectra were corrected by subtraction of the buffer spectrum. A slight fluorescence background was approximated by a polynomial curve.

For the calculation of the sum spectrum, the single-component spectra were normalized to minimize intensity differences to the complex spectrum in the 990-1010 cm^{-1} and 1080–1120 cm^{-1} regions. These regions were selected for the normalization procedure because the intensities of their prominent Raman bands are expected not to change with complex formation. The band at 1003 cm^{-1} is assigned to a phenyl ring breathing vibration, which is protein conformation insensitive (Li et al., 1990). The band at 1092 cm^{-1} is assigned to a phosphate dioxy stretching vibration and is invariant to repressor-operator complex formation (Benevides et al., 1991c).

A difference spectrum was calculated between the complex spectrum and the sum spectrum of the separately measured component spectra. Difference bands are considered as significant when the following criteria are fulfilled: 1) their intensity is at least two times higher than the signal-to-noise ratio, 2) the difference bands reflect intensity changes of at least 5% of their parent bands, and 3) they are observed with both 17-mer and 18-mer operators.

Infrared spectroscopy

Infrared spectra were recorded as described recently, using a Bruker IFS 66 Fourier transform infrared spectrometer equipped with a deuterated triglycine sulfate detector (Fabian et al., 1992). The protein and buffer solutions were placed in a special homemade cell with detachable CaF_2 windows and a path length of 11.9 μm.

RESULTS

Raman spectrum of 17-mer operator

Fig. 2 (*trace 2*) shows the Raman spectrum of the 17-mer operator in the region 600-1720 cm^{-1}. The backbone conformation markers at 831 and 1092 cm^{-1} are typical of B-DNA of this base composition (Thomas and Wang, 1988). The nucleoside conformation markers at 681 cm^{-1} (dG), 728 cm^{-1} (dA), 750 cm^{-1} (dT), and 1256 cm^{-1} (dC) identify C2′-endo/anti-conformers. Peak assignments are included in Table 1. In the Raman spectrum of the 18-mer operator (not shown), thymine bands are more intense because of its higher thymine content.

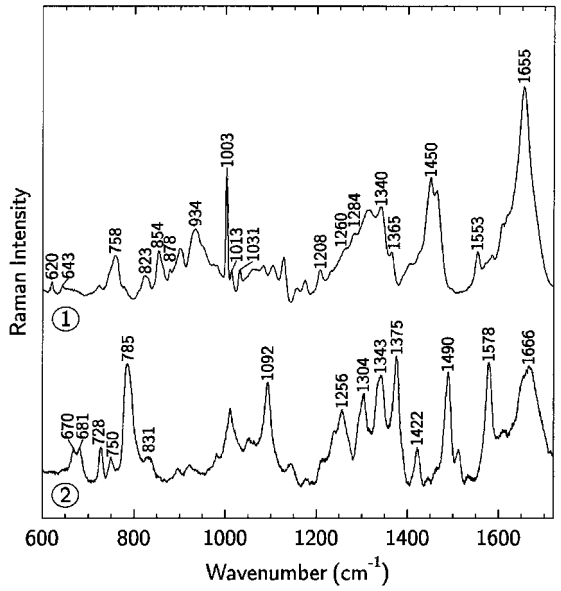

FIGURE 2 Raman spectra of the Tet repressor protein (*trace 1*) and the 17-mer operator (*trace 2*). The TetR spectrum is shifted to avoid overlap. Peak positions of prominent Raman bands are marked in both spectra and are listed in Table 1.

TABLE 1 Prominent Raman bands and peak assignments of Tet repressor and 17-mer operator DNA

Peak	Assignment	Peak	Assignment
620	Phe	1208	Tyr, Phe
643	Tyr	1256	C
670	T	1260	Amide III
681	G	1284	Amide III
728	A	1304	A
750	T	1340	Trp
758	Trp	1343	A
785	C, bk	1365	Trp
823	Tyr	1375	T
831	bk (OPO)	1422	CH_2
854	Tyr	1450	CH_2
878	Trp	1490	G
934	C-C stretch	1553	Trp
1003	Phe	1578	G, A
1013	Trp	1655	Amide I
1031	Phe	1666	T
1092	bk $(PO_2)^-$		

Frequencies (cm^{-1}) are accurate to $\pm$ 2 cm^{-1}. G, guanine; A, adenine; C, cytosine; T, thymine; bk, deoxyribose phosphate backbone; OPO, phosphodiester backbone group; PO_2^-, phosphodioxy backbone group.

Raman spectrum of Tet repressor

Fig. 2 (*trace 1*) shows the Raman spectrum of TetR. It contains bands originating from modes of the peptide backbone, particularly the amide I (1640–1680 cm^{-1}), amide III (1230–1300 cm^{-1}), and the skeletal mode of α-helix (934 cm^{-1}). Other Raman bands are assigned to CH_2 groups of aliphatic side chains (1450 cm^{-1}), tyrosines (643, 823, 854, and 1208 cm^{-1}), tryptophans (758, 878, 1013, 1340, 1365, and 1553 cm^{-1}), and phenylalanines (620, 1003, 1031, and 1208 cm^{-1}). Table 1 summarizes all peak assignments.

Peptide backbone markers of Tet repressor

The amide I and amide III bands are diagnostic of the secondary structure. The major amide I component is centered at ~1655 cm^{-1}, indicating α-helices as the dominant secondary structural elements (Chen and Lord, 1974). The amide III peaks at 1260 and 1284 cm^{-1} and the intense C-C stretch band at 934 cm^{-1}, which are characteristic for helical structures, confirm this conclusion. The low intensity in the amide III region between 1230 and 1240 cm^{-1} is consistent with the absence of substantial amounts of β-structures.

Side-chain environments

Tyrosine. The intensity ratio $R_y = I_{854}/I_{823}$ of the tyrosine peaks at 854 and 823 cm^{-1} is sensitive to hydrogen bonding of the phenolic OH groups (Siamwiza et al., 1975). An R_y value of 2.5 is observed when the phenolic oxygen is the acceptor atom in a strong hydrogen bond for which the proton donor is very acidic hydrogen. R_y is in the range of 1.25 when the phenolic OH acts as both donor and acceptor of moderately strong hydrogen bonds, as, for example, when exposed to solvent H_2O molecules. R_y is as low as 0.3 when OH is the donor of a strong hydrogen bond to a very negative acceptor group, such as a carboxylate ion. From the Raman spectrum of TetR given in Fig. 2, we find that $R_y = 1.9$. This intensity ratio represents an average over hydrogen bonding states of all tyrosines and is consistent with a predominant surface localization of the five tyrosines that are hydrogen bonded to solvent H_2O molecules. This result is in agreement with the hydrogen bonding state of the tyrosines in the crystal structure (Hinrichs et al., 1994).

Tryptophan. The tryptophan indole ring mode near 880 cm^{-1} is diagnostic of the hydrogen bonding strength of the exocyclic 1NH donor (Miura et al., 1988). Without H-bonding at the N1 site, this band is located at 883 cm^{-1}; with strong H-bonding it is located at 871 cm^{-1}. In Fig. 2 the band is observed at 878 cm^{-1}, indicating medium strong hydrogen bonding by 1NH donors of both Trp^{43} and Trp^{75}. The crystal structure of TetR reveals that the solvent-exposed Trp^{43} is H-bonded to water molecules. Although Trp^{75} is buried in a hydrophobic pocket, its 1NH is also H-bonded to H_2O solvent molecules.

The intensity ratio of the tryptophan peaks near 1360 and 1340 cm^{-1}, the Fermi doublet of the indole ring, is diagnostic of the hydropathicity of the ring environment (Harada et al., 1986). The weak peak at 1365 cm^{-1} indicates relatively hydrophilic indole ring environments, reflecting the solvent accessibility of Trp^{43} and Trp^{75} mentioned above.

The frequency of the Trp vibration near 1550 cm^{-1} varies from 1542 to 1557 cm^{-1} as a function of the absolute value of the $C_\alpha C_\beta$-C_3C_2 torsion angle $|\chi^{2,1}|$ in the range 60°-120° (Miura et al., 1989). According to this relationship, the position at 1553 $\pm$ 1 cm^{-1} indicates an average angle of

$|\chi^{2,1}| \approx 99° \pm 3°$ over both Trp side chains. This is in excellent agreement with the crystal structure, which shows an average angle of 96° with $|\chi^{2,1}|$ values of 95° and 97° for Trp^{43} and Trp^{75}, respectively.

Raman spectrum of Tet repressor:[Ni-tetracycline]$^+$

Fig. 3 shows the Raman spectrum of TetR:[Ni-Tc]$^+$ (*trace 1*), the spectral difference of TetR:[Ni-Tc]$^+$ minus TetR (*trace 2*), the spectrum of free Tc (*trace 3*), and the difference spectrum, enlarged two times, of TetR:[Ni-Tc]$^+$ minus the sum of the separately measured spectra of TetR and Tc (*trace 4*). Trace 2 corresponds to the spectrum of bound Tc.

Bands assigned to Tc dominate, although the Tc concentration in the sample is only ~0.2 μg/μl. This might be a preresonance effect. Tc has a maximum of absorption at 382 nm, and there is significant residual absorption at the excitation wavelengths of 488 and 514.5 nm used for the measurements. For Tc-containing samples, three spectral scans of 10 s each were averaged at four spectrometer positions to avoid optical degradation of the light-sensitive Tc.

Some Tc peaks were tentatively assigned after measuring Raman spectra in H_2O and D_2O. The band near 1617 cm^{-1} is typical for C═O stretching vibrations. The band positioned around 1404 cm^{-1} in H_2O shifts to 1394 cm^{-1} in D_2O. This indicates the involvement of hydrogens and suggests an assignment of this band to N-CH_3 deformation vibrations. The intense bands between 1230 and 1360 cm^{-1} are located in the region of C-C and C-N stretching vibrations and shift to higher wavenumbers in D_2O, whereas no significant wavenumber shifts were observed for the bands at 1178 cm^{-1} and 1436 cm^{-1}.

Difference peaks (Fig. 3, *trace 4*) can be assigned to Tc, but there are no hints for conformational changes of TetR after [Ni-Tc]$^+$ binding. In the bound state the Tc band at 1250 cm^{-1} becomes sharper, the 1285 cm^{-1} and 1599 cm^{-1} bands increase, the 1310 cm^{-1} band is broader, and the intensity ratio 1404/1436 increases (compare Fig. 3, *traces 2* and *3*). The change in the shape of the 1250 cm^{-1} band signifies a more uniform conformation of the corresponding group. The interactions between TetR and Tc involve hydrogen bonds and hydrophobic interactions, as identified in the x-ray crystal structure (Hinrichs et al., 1994). Ring D of Tc is mainly involved in hydrophobic interactions, ring A is mostly responsible for hydrogen bonding, and rings B and C interact with the cation.

Fourier transform infrared spectrum of Tet repressor

Fig. 4 shows infrared spectra of free TetR and of TetR:[Ni-Tc]$^+$ in the wavenumber range of 1750–1500 cm^{-1} measured in D_2O. The spectra are nearly identical in the amide I′ region; very minor differences below 1600 cm^{-1} are within the experimental error. The peak positions are found at 1652 cm^{-1}, as expected for proteins composed of α-helical secondary structure elements (Byler and Susi, 1986; Surewicz and Mantsch, 1988), and are consistent with the results of the x-ray structural determination (Kisker et al., 1995). Similar results were obtained by measuring IR spectra of TetR in H_2O, in both the presence and absence of [Ni-Tc]$^+$ (data not shown).

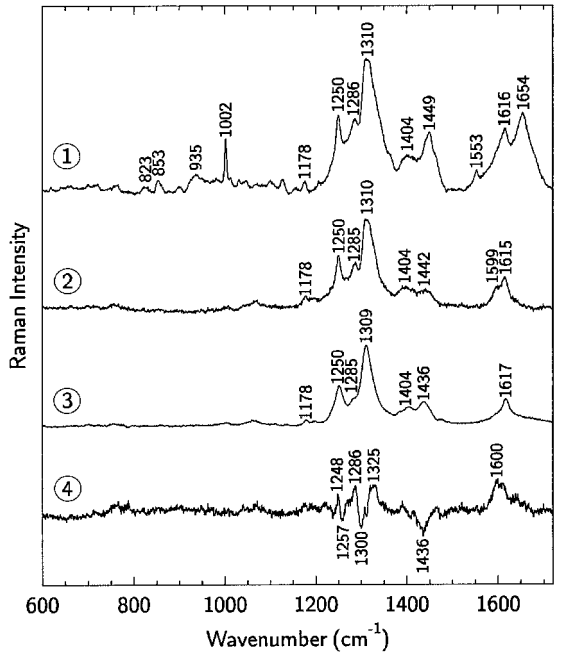

FIGURE 3 Raman spectrum of the Tet repressor:tetracycline-Ni^{2+} complex (*trace 1*), difference spectrum TetR:[Ni-Tc]$^+$ minus TetR (*trace 2*), spectrum of free tetracycline (*trace 3*), and difference spectrum, enlarged two times, of TetR:[Ni-Tc]$^+$ minus the sum of the separately measured spectra of TetR and Tc (*trace 4*).

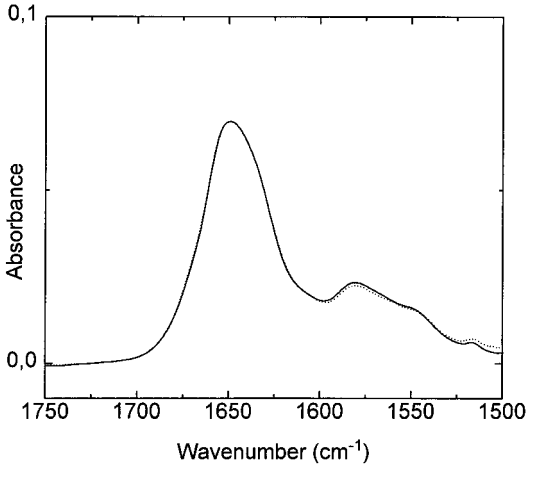

FIGURE 4 Infrared spectra of Tet repressor (——) and TetR:[Ni-Tc]$^+$ (·····) in the region 1750 cm^{-1} to 1500 cm^{-1}.

Raman spectrum of Tet repressor:operator complex

Fig. 5 shows the Raman spectrum of the TetR:17-mer operator DNA complex (*trace 1*), the computed sum of the separately measured component spectra (*trace 2*), and the difference spectrum of complex minus constituents (*trace 3*). A difference spectrum that has been enlarged four times is shown for easier recognition of difference bands (*trace 4*). As a control, the difference spectrum (enlarged four times) of a mixture of TetR:$[Ni\text{-}Tc]^+$ and operator DNA minus the sum of the separately measured component spectra is included (*trace 5*).

Positions of the Raman peaks of the TetR:17-mer operator DNA complex, except for the 781 cm^{-1} peak, and the components (Table 1) agree within an uncertainty of 1 cm^{-1} for sharp and 2 cm^{-1} for broader peaks. Difference bands (Fig. 5, *traces 3* and *4*) provide information about conformational changes and interactions that accompany complex formation.

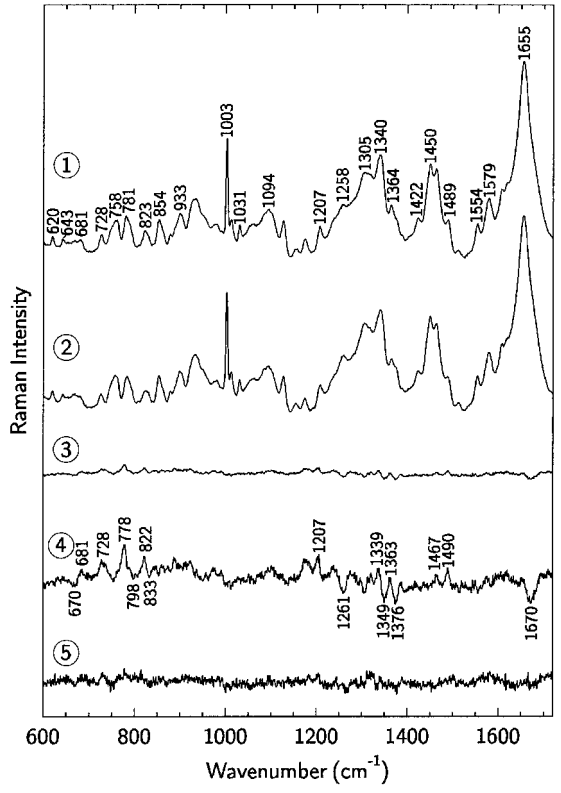

FIGURE 5 (*Trace 1*) Raman spectrum of the Tet repressor:17-mer operator complex. (*Trace 2*) Sum of the spectra of the isolated components shown in Fig. 2. (*Trace 3*) Difference between the experimental spectrum of the Tet repressor:17-mer operator complex and the sum of the component spectra. (*Trace 4*) Difference spectrum shown in trace 3, enlarged four times. (*Trace 5*) Difference spectrum, enlarged four times, between the experimental spectrum of a mixture of TetR:$[Ni\text{-}Tc]^+$ with 18-mer operator and the sum of the component spectra.

Effects on DNA Raman bands induced by complex formation

A Raman peak at 670 cm^{-1} is assigned to thymine. The thymine peak overlaps with a guanine peak at 681 cm^{-1} and is therefore not well resolved in the spectra shown in Fig. 5 (*traces 1* and *2*). A negative band at 670 cm^{-1} in the difference spectrum (Fig. 5, *trace 4*) indicates decreased intensity in the complex.

The 681 cm^{-1} peak is a conformation marker of guanine nucleosides characteristic for B-DNA. The positive difference band at 681 cm^{-1} shows increased intensity of the dG vibration in the complex.

The peaks at 728 and 781 cm^{-1} (Fig. 5, *trace 1*) are assigned to in-phase ring breathing vibrations of adenine and cytosine base residues, respectively. These peaks show increased intensity upon complex formation, as indicated by positive difference bands at 728 and 778 cm^{-1}.

The cytosine peak at 781 cm^{-1} overlaps a backbone component around 798 cm^{-1}. The 798 cm^{-1} band is assigned to a stretching vibration of backbone phosphodiester groups and shows reduced intensity in bound DNA. With increased cytosine intensity at 778 cm^{-1} and decreased intensity at 798 cm^{-1}, the maximum of the peak resulting from the two overlapping bands shifts from 785 cm^{-1} for free DNA (Fig. 2, *trace 2*) to 781 cm^{-1} for the complex (Fig. 5, *trace 1*). A small negative difference peak at 833 cm^{-1} is found in Fig. 5 (*trace 4*). Raman intensity decreases near 795 and 830 cm^{-1} and an intensity increase near 776 cm^{-1} accompany changes in B-DNA backbone geometry (Erfurth and Peticolas, 1975; Benevides et al., 1991a). The DNA bands at 795 and 830 cm^{-1} were correlated with phosphodiester torsion angles configured as in the B-form of DNA. The observed intensity decrease of these bands is consistent with subtle distortions induced in the B-DNA backbone geometry by TetR binding.

Raman bands in the interval 1250–1750 cm^{-1} are sensitive to specific interactions between DNA bases and major groove-binding proteins. A Raman marker of DNA-protein interactions is the dG band near 1490 cm^{-1}, which shifts to ~1470 cm^{-1} upon hydrogen bond donation to the guanine ring N7 acceptor (Hartman et al., 1973; Nishimura et al., 1986; Benevides et al., 1991b,c, 1994a,b). Therefore, hydrogen bonding to guanine N7 should cause a positive band at 1467 cm^{-1} and a negative band at 1490 cm^{-1} in the difference spectrum. Unstacking of bases or changes in the stacking geometry, however, would result in an intensity increase at 1490 cm^{-1} (Erfurth and Peticolas, 1975) and overlap the intensity decrease expected in the case of hydrogen bonding. In fact, the difference spectrum shows positive bands at 1467 and 1490 cm^{-1}. Most probably, the positive band at 1467 cm^{-1} reflects hydrogen bonding of guanine N7 acceptors to TetR donor groups in the complex, and the positive band at 1490 cm^{-1} is caused by effects of unstacking or changes in the stacking geometry.

A Raman peak at 1376 cm^{-1} is assigned to the thymine 5-CH_3 group; the negative difference band at this position

indicates decreased Raman intensity in the TetR:operator complex. An increased Raman intensity at 1376 cm^{-1} was correlated with hydrophobic interaction between a thymine 5-CH_3 group and an aliphatic side chain (Benevides et al., 1991b,c). However, in the TetR:operator complex, this intensity decreases, as also observed recently for the complex of phage D108 Ner repressor with a 61-bp operator DNA (Benevides et al., 1994a). The effect was interpreted by Benevides et al. (1994a) as an increased solvent accessibility of thymine 5-CH_3 groups in the complex in comparison to the protein-free *ner* operator.

Effects on Raman bands of TetR induced by complex formation

The Raman intensity ratio $R_y = I_{854}/I_{823}$, which is diagnostic of the H-bonding environment of tyrosines, decreases from 1.9 in the spectrum of free TetR to 1.6 in the spectrum of complexed TetR. The spectrum of complexed TetR was approximated by subtraction of the operator DNA spectrum from the complex spectrum. To check the compensation of DNA contributions in the regions near the tyrosine bands, the quotient $I_{643}/(I_{823} + I_{854})$ was calculated. Examination of Raman spectra of a large number of proteins indicated that the quotient falls within the narrow range 0.24 ± 0.018 (Benevides et al., 1991a, and references therein). For free and complexed TetR, values between 0.22 and 0.23 were found, confirming the assignment of the difference band at 822 cm^{-1} to tyrosine. Thus DNA does not contribute significantly to the difference band around 822 cm^{-1}.

The decrease in the intensity ratio R_y is consistent with a more hydrophobic environment of one or more tyrosine residues in the complex. The spectroscopic data alone cannot identify the involved tyrosines. One candidate for an interaction with the operator is Tyr^{42}, located in the recognition helix of the HTH motif.

Aromatic ring vibrations of phenylalanine and tyrosine contribute to the Raman peak at 1207 cm^{-1}. The positive band in the difference spectrum indicates an increased intensity at this position of the complex spectrum and probably reflects tyrosine binding to the operator, but it is not possible to establish this correlation because contributions of phenylalanine cannot be excluded.

The tryptophan peak at 1364 cm^{-1} increases after complex formation, causing a positive difference band at 1363 cm^{-1} (Fig. 5, *trace 4*). It is known from the x-ray structure of TetR that Trp^{43} is located near the end of the recognition helix and is solvent exposed. An increase in the 1364 cm^{-1} peak points to a reduced hydrophilicity of the indole ring environment and is consistent with a contact between Trp^{43} and the operator.

The negative difference bands around 1670 and 1261 cm^{-1} are close to the amide I and amide III regions, respectively, and probably reflect changes in the secondary structure of TetR. The negative difference band in the amide I region may reflect a small decrease in ordered secondary structure. The amide I trough represents ~5% of the parental band intensity, suggesting that the conformation of only a few residues is perturbed by DNA binding. The difference bands at 1670 cm^{-1} and 1261 cm^{-1}, however, also coincide with a thymine and a cytosine band, respectively. Therefore, contributions from thymine and cytosine cannot be excluded.

In the difference spectrum a positive band at 1339 cm^{-1} and a negative band at 1349 cm^{-1} are found. This feature is assigned to the conformation of aliphatic amino acid side chains (Li et al., 1990), consistent with a contact of Pro^{39} with base pairs 4 and 5.

Raman spectrum of a mixture of TetR:$[Ni\text{-}Tc]^+$ and operator DNA

Raman spectra of TetR:$[Ni\text{-}Tc]^+$, operator DNA, and a mixture of the two components in 1:1 molar ratio were measured. The Raman spectrum of the mixture and the computed sum of the separately measured component spectra are nearly identical. The difference spectrum of these two spectra is shown in Fig. 5 (*trace 5*). The spectral features of trace 5 do not exceed the experimental error. All of the spectral features labeled in Fig. 5, trace 4, and discussed above are missing from trace 5. This result indicates that TetR:$[Ni\text{-}Tc]^+$ and operator DNA do not influence each other under the experimental conditions. It was expected from the well-known inducer effect of tetracycline-metal ion complexes (Hillen and Berens, 1994) that TetR:$[Ni\text{-}Tc]^+$ does not bind to operator DNA. The absence of spectroscopic effects confirms this expectation, despite the high concentrations necessary for the Raman experiment.

Furthermore, the result indicates that any effects of Ni^{2+} or $[Ni\text{-}Tc]^+$ on operator DNA are missing. These ions might be present in the sample when the components could not be mixed in a molar ratio of exactly 1:1, because of experimental limitations. Ni^{2+} ions induce structural changes in DNA, as shown by laser Raman spectroscopy at metal:phosphate molar ratios of 0.6:1 (Duguid et al., 1993). In our experiment, however, the concentration of Ni^{2+} is much lower. The metal:phosphate molar ratio is only 0.028:1 when the total Ni^{2+} concentration is considered. Because a tetracycline:Ni^{2+} molar ratio of 1:1 was used and an association constant in the nanomolar range can be expected, the concentration of free Ni^{2+} is obviously far too low for the induction of measurable effects on DNA.

DISCUSSION

Raman spectra are indicative for DNA backbone conformation, base contacts, aromatic amino acid side-chain environments, and protein secondary structure. The aim of this study is a Raman spectroscopic characterization of the interaction between the DNA-binding protein TetR, utilizing the HTH motif, and operator DNA. For this purpose, the

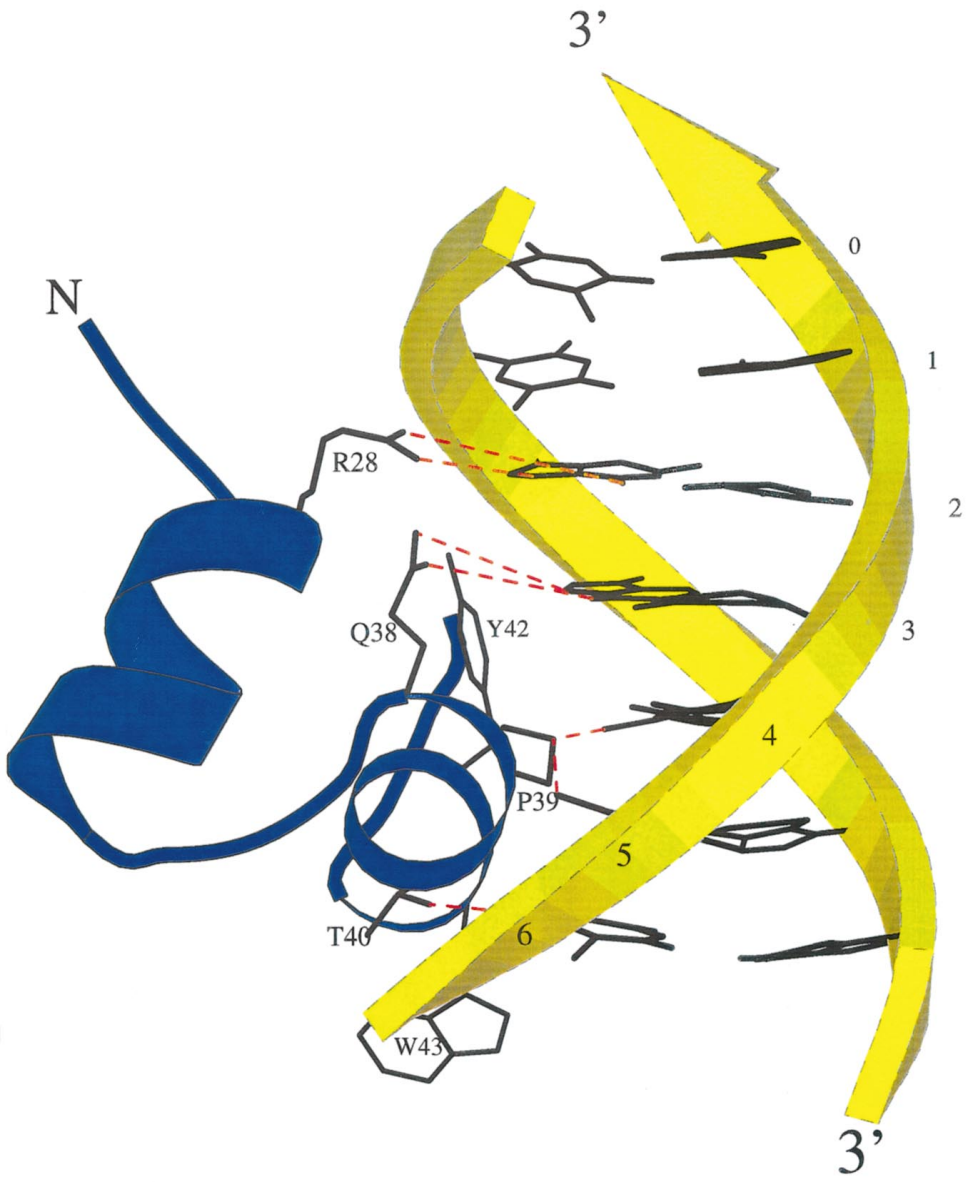

FIGURE 6 Schematic view of a part of the TetR:operator DNA complex, showing the helix-turn-helix motif of $TetR^D$ and 7 bp of operator O1 half-site. The plot is based on preliminary data of a crystal structure analysis of the complex (Orth et al., unpublished observation) and was produced with the program MOLSCRIPT (Kraulis, 1991). Base pairs are numbered as given in Fig. 1, starting with 0 for the central T · A base pair. Amino acids R28, Q38, P39, T40, Y42, and W43 are labeled. The arrows point in the 5′ to 3′ direction of the DNA backbone.

spectra of the isolated components and the complex were measured. Raman difference spectra were calculated by subtracting the sum spectrum of the components from the experimental spectrum of the complex.

Two aspects of the work should be recognized. First, the available knowledge derived from biochemical, microbiological, and genetic experiments provides a background for the interpretation of the Raman bands. This enables us to confirm and strengthen published correlations and assignments of spectral effects and structural properties obtained from studies of other systems. Thus our results contribute to the general methodological development. Second, we obtained direct physicochemical evidence for conclusions drawn from microbiological and genetic experiments. The results support the ongoing x-ray structural analysis and contribute independent data to the emerging model of TetR and its complex with operator DNA.

In the difference spectrum of a mixture of TetR:$[Ni\text{-}Tc]^+$ and operator DNA minus the sum of the components, no significant spectral features were observed. This Raman spectroscopic result confirms that the TetR:$[Ni\text{-}Tc]^+$ complex does not bind to operator DNA.

The Raman difference spectrum between the TetR:operator DNA complex and the sum of the experimental spectra of TetR and operator DNA indicates small changes in the operator DNA phosphate backbone conformation, and some difference bands provide clear evidence for contacts of nucleic acid bases with protein groups. They characterize

the participation of thymine methyl groups, guanine N7 atoms, and aromatic ring systems of adenine and cytosine. After complex formation, some tyrosine and tryptophan residues are in a more hydrophobic environment. The observed differences in the conformation-sensitive amide bands of TetR are consistent with changes in the polypeptide backbone structure of TetR. This might be connected with complex formation, requiring a reduction of the distance between the DNA-binding helices in the HTH motifs.

Altered base stacking is expected to accompany changes in DNA backbone torsions (Benevides et al., 1991a, 1994a,b). The Raman effects observed for the TetR:operator complex are consistent with this expectation: difference peaks and troughs observed between 650 and 780 cm^{-1} probably reflect changes in DNA base stacking, and distortions of B-DNA backbone torsions are indicated by the negative difference peaks at 798 and 833 cm^{-1} (Fig. 5, *trace 4*). TetR binding induces curvature in operator O1 and O2 DNA containing more than 70 bp. This was concluded from gel mobility electrophoresis, circular dichroism, neutron scattering, and electrooptical studies (Tovar and Hillen, 1989). However, the Raman data obtained here for a 17-bp operator DNA neither add further evidence nor argue against DNA curvature.

Infrared and Raman spectra of free TetR and TetR in complex with $[Ni\text{-}Tc]^+$ do not indicate conformational changes of the protein caused by Tc binding. This is in agreement with the results of a crystal structure determination of TetR in the absence of Tc (Kisker, 1994), which showed the same distance of 39 Å between the recognition helices as in the TetR:$[Mg\text{-}Tc]^+$ complex (Hinrichs et al., 1994; Kisker et al., 1995).

Fig. 6 shows a schematic view of a part of the TetR:operator complex, with the HTH binding region of the protein and a half-site of the operator DNA, based on preliminary data of the crystal structure analysis of the complex (Orth et al., unpublished observations). Baumeister et al. (1992) proposed from genetic experiments the following contacts between TetR monomer and the major groove of the operator half-site: 1) Arg^{28} contacts guanine of the base pair at position 2 with two H-bonds; 2) Gln^{38} binds adenine of the A · T base pair at position 3 with two H-bonds; 3) Pro^{39} inserts its side chain between the thymine methyl groups of T · A and A · T base pairs at positions 4 and 5; 4) the methyl group of Thr^{40} participates in a van der Waals contact to cytosine of the G · C base pair at position 6.

The knowledge derived from the experiments mentioned above provides a background for the discussion of the Raman data. These data are consistent with several details of the model shown in Fig. 6: 1) the positive difference band at 1467 cm^{-1} assigned to hydrogen bond formation of the guanine N7 acceptor is consistent with Arg^{28} contacts with guanine of the G · C base pair at position 2; 2) the positive difference band at 1363 cm^{-1} indicates a more hydrophobic environment of Trp and is consistent with DNA interaction of Trp^{43}, located near the C-terminal end of the recognition helix; 3) the positive difference band at 1339 cm^{-1} and the negative band at 1349 cm^{-1} assigned to Pro, and a band at 1376 cm^{-1} assigned to thymine are suggestive for the contact of Pro^{39} with base pairs 4 and 5; 4) a positive difference band at 822 cm^{-1} assigned to Tyr, as well as a decrease in the Raman intensity ratios $R_y = I_{854}/I_{823}$, is consistent with a more hydrophobic environment of Tyr^{42} of the recognition helix in the TetR:operator complex; 5) the positive difference band at 728 cm^{-1} assigned to adenine may correlate with interactions of Gln^{38} at position 3; 6) the positive difference band at 778 cm^{-1} assigned to cytosine possibly reflects the contact with Thr^{40} at position 6.

In summary, the Raman data are consistent with the available biochemical, molecular biological, and crystallographic data on TetR and on the TetR:operator complex. They provide additional spectroscopic evidence and extend our understanding of this system in the solution state.

We thank Prof. W. Hillen for providing the *E. coli* TetR overproducer strain, and we are grateful to Claudia Alings and Heike Roscher for expert technical assistance. We thank the reviewers for helpful comments.

The work was supported by the Deutsche Forschungsgemeinschaft through Sonderforschungsbereich 344 and Graduiertenkolleg "Modellstudien zu Struktur, Eigenschaften und Erkennung biologischer Moleküle auf atomarer Ebene," and by Fonds der Chemischen Industrie.

REFERENCES

Baumeister, R., V. Helbl, and W. Hillen. 1992. Contacts between Tet repressor and *tet* operator revealed by new recognition specificities of single amino acid replacement mutants. *J. Mol. Biol.* 226:1257–1270.

Benevides, J. M., G. Kukolj, C. Autexier, K. L. Aubrey, M. S. DuBow, and G. J. Thomas, Jr. 1994a. Secondary structure and interaction of phage D108 Ner repressor with a 61-base-pair operator: evidence for altered protein and DNA structure in the complex. *Biochemistry.* 33: 10701–10710.

Benevides, J. M., P. L. Stow, L. Ilag, N. L. Incardona, and G. J. Thomas, Jr. 1991a. Differences in secondary structure between packaged and unpackaged single-stranded DNA of bacteriophage ΦX174 determined by Raman spectroscopy: a model for ΦX174 DNA packaging. *Biochemistry.* 30:4855–4863.

Benevides, J. M., M. A. Weiss, and G. J. Thomas, Jr. 1991b. Design of the helix-turn-helix motif: nonlocal effects of quaternary structure in DNA recognition investigated by laser Raman spectroscopy. *Biochemistry.* 30:4381–4388.

Benevides, J. M., M. A. Weiss, and G. J. Thomas, Jr. 1991c. DNA recognition by the helix-turn-helix motif: investigation by laser Raman spectroscopy of the phage λ repressor and its interaction with operator sites O_L1 and O_R3. *Biochemistry.* 30:5955–5963.

Benevides, J. M., M. A. Weiss, and G. J. Thomas, Jr. 1994b. An altered specificity mutation in the λ repressor induces global reorganization of the protein-DNA interface. *J. Biol. Chem.* 269:10869–10878.

Byler, D. M., and H. Susi. 1986. Examination of the secondary structure of proteins by deconvolved FTIR spectra. *Biopolymers.* 25:469–487.

Chen, M. C., and R. C. Lord. 1974. Laser-excited Raman spectroscopy of biomolecules. VI. Some polypeptides as conformational models. *J. Am. Chem. Soc.* 96:4750–4752.

Duguid, J., V. A. Bloomfield, J. M. Benevides, and G. J. Thomas, Jr. 1993. Raman spectroscopy of DNA-metal complexes. I. Interactions and conformational effects of the divalent cations: Mg, Ca, Sr, Ba, Mn, Co, Ni, Cu, Pd, and Cd. *Biophys. J.* 65:1916–1928.

Erfurth, S. C., and W. L. Peticolas. 1975. Melting and premelting phenomenon in DNA by laser Raman scattering. *Biopolymers.* 14:247–264.

Ettner, N., J. W. Metzger, T. Lederer, J. D. Hulmes, C. Kisker, W. Hinrichs, G. A. Ellestad, and W. Hillen. 1995. Proximity mapping of the Tet repressor-tetracycline-Fe^{2+} complex by hydrogen peroxide mediated protein cleavage. *Biochemistry.* 34:22–31.

Ettner, N., G. Müller, C. Berens, H. Backes, D. Schnappinger, T. Schreppel, K. Pfleiderer, and W. Hillen. 1996. Fast large-scale purification of tetracycline repressor variants from overproducing *Escherichia coli* strains. *J. Chromatogr. A.* 742:95–105.

Fabian, H., D. Naumann, R. Misselwitz, O. Ristau, D. Gerlach, and H. Welfle. 1992. Secondary structure of streptokinase in aqueous solution: a Fourier transform infrared spectroscopic study. *Biochemistry.* 31: 6532–6538.

Harada, I., T. Miura, and H. Takeuchi. 1986. Origin of the doublet at 1360 and 1340 cm^{-1} in the Raman spectra of tryptophan and related compounds. *Spectrochim. Acta.* 42A:307–312.

Hartman, K. A., R. C. Lord, and G. J. Thomas, Jr. 1973. Structural studies of nucleic acids and polynucleotides by infrared and Raman spectroscopy. *In* Physicochemical Properties of Nucleic Acids, Vol. 1. J. Duchesne, editor. Academic Press, New York. 1–89.

Helbl, V., C. Berens, and W. Hillen. 1995. Proximity probing of Tet repressor to *tet* operator by dimethylsulfate reveals protected and accessible functions for each recognized base-pair in the major groove. *J. Mol. Biol.* 245:538–548.

Hillen, W., and C. Berens. 1994. Mechanisms underlying expression of Tn*10* encoded tetracycline resistance. *Annu. Rev. Microbiol.* 48: 345–369.

Hinrichs, W., C. Kisker, M. Düvel, A. Müller, K. Tovar, W. Hillen, and W. Saenger. 1994. Structure of the Tet repressor-tetracycline complex and regulation of antibiotic resistance. *Science.* 264:418–420.

Kaneko, M., A. Yamaguchi, and T. Sawai. 1985. Energetics of tetracycline efflux system encoded by Tn*10* in *Escherichia coli. FEBS Lett.* 193: 893–899.

Kisker, C. 1994. Antibiotics resistance: x-ray structure analysis of the tetracycline repressor and molecular mechanism of the resistance regulation. Ph.D. thesis. Freie Universität, Berlin.

Kisker, C., W. Hinrichs, K. Tovar, W. Hillen, and W. Saenger. 1995. The complex formed between Tet repressor and tetracycline-Mg^{2+} reveals mechanism of antibiotic resistance. *J. Mol. Biol.* 247:260–280.

Kraulis, P. J. 1991. Molscript: a program to produce both detailed and schematic plots of protein structures. *J. Appl. Crystallogr.* 24:946–950.

Li, T., Z. Chen, J. E. Johnson, and G. J. Thomas, Jr. 1990. Structural studies of bean pot mottle virus, capsid, and RNA in crystal and solution states by laser Raman spectroscopy. *Biochemistry.* 29:5018–5026.

Miura, T., H. Takeuchi, and I. Harada. 1988. Characterization of individual tryptophan side chains in proteins using Raman spectroscopy and hydrogen-deuterium exchange kinetics. *Biochemistry.* 27:88–94.

Miura, T., H. Takeuchi, and I. Harada. 1989. Tryptophan Raman bands sensitive to hydrogen bonding and side-chain conformation. *J. Raman Spectrosc.* 20:667–671.

Nishimura, Y., M. Tsuboi, T. Sato, and K. Akoi. 1986. Conformation-sensitive Raman lines of mononucleotides and their use in a structure analysis of polynucleotides: guanine and cytosine nucleotides. *J. Mol. Struct.* 146:123–153.

Orth, P., C. Alings, D. Schnappinger, W. Saenger, and W. Hinrichs. 1998. Crystallization and preliminary analysis of the Tet-repressor/operator complex. *Acta Crystallogr. D.* 54 (In press).

Peviani, C., W. Hillen, N. Ettner, H. Lami, S. M. Doglia, E. Piemont, C. Ellouze, and M. Chabbert. 1995. Spectroscopic investigation of Tet repressor tryptophan-43 upon specific and nonspecific DNA binding. *Biochemistry.* 34:13007–13015.

Siamwiza, M. N., R. C. Lord, M. C. Chen, T. Takamatsu, I. Harada, H. Matsuura, and T. Shimanouchi. 1975. Interpretation of the doublet at 850 and 830 cm^{-1} in the Raman spectra of tyrosyl residues in proteins and certain model compounds. *Biochemistry.* 14:4870–4876.

Surewicz, W. K., and H. H. Mantsch. 1988. New insight into protein secondary structure from resolution-enhanced infrared spectra. *Biochim. Biophys. Acta.* 952:115–130.

Thomas, G. J., Jr., and M. Tsuboi. 1993. Raman spectroscopy of nucleic acids and their complexes. *Adv. Biophys. Chem.* 3:1–70.

Thomas, G. J., Jr., and A. H.-J. Wang. 1988. Laser Raman spectroscopy of nucleic acids. *Nucleic Acids Mol. Biol.* 2:1–30.

Tovar, K., and W. Hillen. 1989. Tet repressor binding induced curvature of *tet* operator DNA. *Nucleic Acids Res.* 17:6515–6521.

Yamaguchi, A., T. Udagawa, and T. Sawai. 1990. Transport of divalent cations with tetracycline as mediated by the transposon Tn*10*-encoded tetracycline resistance protein. *J. Biol. Chem.* 265:4809–4813.